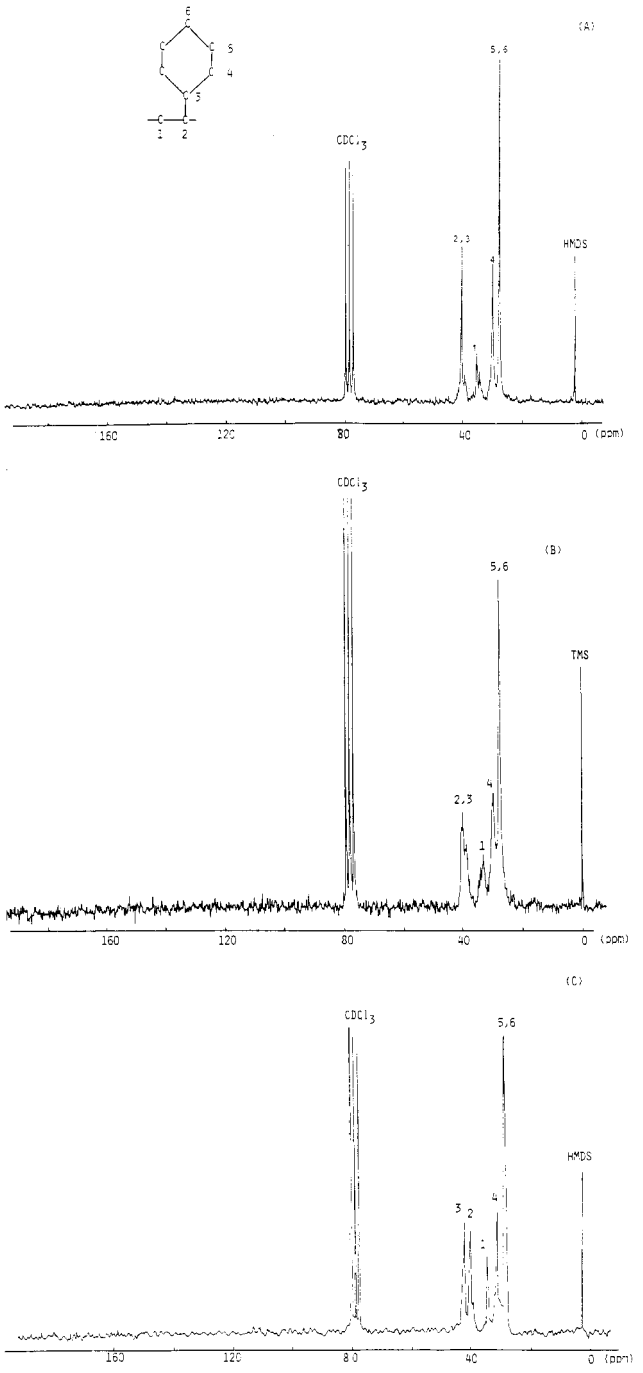

Figure 1. ^{13}C NMR spectra of PVCH. (A) syndiotactic; (B) atactic; (C) isotactic.

weight-average molecular mass (MW) and polydispersity (M_w/M_n) of the syndiotactic PVCH were 6600 based on PS and 2.8. The molecular weight of the hydrogenated polymer seems to be somewhat lower, but it is uncertain at present whether degradation takes place during hydrogenation or not since we have no calibration curve for the molecular mass between PVCH and PS. Figure 2 illustrates the TG–DTA diagram for the syndiotactic PVCH, which indicates that the polymer begins to decompose near 400 °C. This decomposition temperature seems to be higher than those of atactic (368 °C) and isotactic PVCH (379 °C).[8] The glass transition temperature (T_g) of the syndiotactic PVCH determined by DSC was approximately −2.5 °C. If the polymer is crystalline, the melting temperature (T_m) can be estimated to be in the range between 132 and 270 °C from the correlation $^2/_3 < T_g/T_m < {}^1/_2$. The absence of any peak in this range

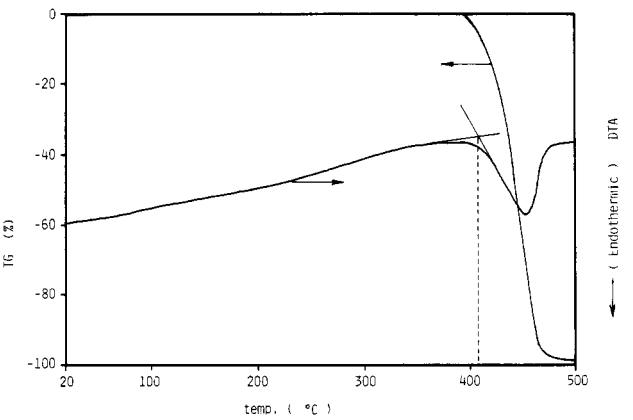

Figure 2. TG–DTA curve of syndiotactic PVCH. Sample weight, 9.03 mg.

(Figure 2) may suggest that this polymer is not crystalline but amorphous.

Additional work is under way to characterize the syndiotactic PVCH more completely, and the results will be reported in another paper.

Registry No. $Ni(NO_3)_2$, 13138-45-9.

References and Notes

(1) Ketley, A. D.; Ehring, R. J.; Fhring, J. *J. Polym. Sci.* **1964**, *A-2*, 755.
(2) Elias, H. G.; Etter, O. *J. Macromol. Sci.* **1967**, *A1-5*, 943.
(3) Ishihara, N.; Seimiya, T.; Kuramoto, M.; Uoi, M. *Macromolecules* **1986**, *19*, 2464.
(4) Pellecchia, C.; Longo, P.; Gassi, A.; Ammendola, P.; Zambelli, A. *Makromol. Chem., Rapid Commun.* **1987**, *8*, 277.
(5) Zambelli, A.; Longo, P.; Pellecchia, C.; Gassi, A. *Macromolecules* **1987**, *20*, 2037.
(6) Sinn, H.; Kaminsky, W.; Vollmer, H. J.; Woldt, R. *Angew. Chem., Int. Ed. Engl.* **1980**, *19*, 390.
(7) Ammendola, P.; Tancredi, T.; Zambelli, A. *Macromolecules* **1986**, *19*, 307.
(8) Helbig, M.; Inoue, H.; Vogl, O. *J. Polym. Sci., Polym. Symp.* **1978**, *63*, 329.

Kazuo Soga,* Hisayuki Nakatani, and Takesi Shiono
Research Laboratory of Resources Utilization, Tokyo Institute of Technology, 4259, Nagatsuta, Midori-ku Yokohama 227, Japan

Received July 18, 1988;
Revised Manuscript Received December 30, 1988

Temperature Ramped Fluorescence Photobleaching Recovery for the Direct Evaluation of Thermoreversible Gels

This communication concerns identification and certain fundamental quantities of reversible gels. Ferry defines a gel as "a substantially dilute solution which does not exhibit steady-state flow".[1] However, identification of gels is complicated by issues of time and spatial extent. For example, a large gel turned on its side might slowly yield to the force of gravity, appearing to flow, while a smaller gel sample of identical composition might exhibit no flow on any experimentally convenient time scale. Also, it can be difficult to distinguish a very viscous solution from a true gel in any reasonable amount of time by macroscopic methods. Even sophisticated rheological measurements do not remove the fundamental problems of mechanical perturbation and time scale from macroscopic flow measurements. There is a need for sensitive, rapid, and non-

0024-9297/89/2222-1500$01.50/0

perturbing methods to identify and characterize gels.

The implication of the Ferry definition is the existence in gels of a spatially filling, three-dimensional network which, though it may be broken even by virtually imperceptible forces or destroyed by heat or other agent, is otherwise permanent. Experiments which test for the existence of a network are direct indicators of gelation, as are rheological methods which test for the absence of flow. Many other tools used to follow gelation are not direct in the sense that they detect neither the absence of flow nor the existence of a network. For example, light scattering is sensitive to all structures, not just the network. Networks have been visualized directly in certain wet gels,[2] and improvements in video optical microscopy and environmental electron microscopy may eventually make visualization possible in many systems. Meanwhile, the existence of a network can be detected via diffusivity measurements; polymers in a network should be immobile. A number of sensitive mobility methods have been developed recently,[3] largely intended for such torpid systems as concentrated solutions, melts, and even bulk polymers.

Chang and Yu were the first to apply one such method, forced Rayleigh scattering (FRS), to a reversible gel, gelatin.[4] A partial decay of the FRS signal was evident, possibly indicating that some gelatin was mobile—i.e., not included in the network structure. Additional measurements by this same group suggest that the number of molecules in this "sol fraction" depends on the age of the gel[5] and may generally be small. Recently, Lee et al. made FRS measurements on atactic polystyrene in CS_2, a system that appears to gel at low temperatures.[6] They find that substantial polymer mobility persists in the gel state. These results demonstrate the new insights that mobility measurements can bring to the study of reversible gels.

We present another mobility-based method for direct gel characterization. Temperature ramped fluorescence photobleaching recovery (TRFPR), an extension of the fluorescence photobleaching recovery (FPR) technique,[7-11] is designed to rapidly and directly determine gel melting points, sol fraction, and mobility of the molecules in the sol, all with zero mechanical perturbation and minimal perturbation of any kind. TRFPR (and FPR) can be applied to a wide variety of gels, requiring only the covalent attachment of a dye if the polymer does not already contain photobleachable fluorophores. The methods are attractive for the study of precious samples, or for studies of the homogeneity of larger samples, as the measured volume is less than 2 μL. In this paper, the TRFPR method is demonstrated provisionally using gelatin gels. This is not an exhaustive study of gelatin but only a demonstration of the new opportunities in reverisble gel research provided by the TRFPR and FPR methods.

Description of the Method. FPR. In the usual FPR method,[7-9] a small spot in a sample is illuminated by a weak laser beam which substitutes for the epi-illuminator of an optical microscope. In the case where a Ronchi ruling (a glass with equal clear and black stripes) is placed in the rear focal plane of the objective, a fringed spot with equal dark and bright stripes appears in the sample. The fluorescence intensity from the bright strips is measured. To initiate a mobility measurement, the laser intensity is dramatically increased for a short period, permanently bleaching some of the fluorophores. Thus, when the laser intensity is returned to its initial low value, it is found that the fluorescence is reduced. As molecules from the bright and dark regions exchange by diffusion, the fluorescence returns at a rate proportional to the tracer self-diffusivity, D. This exchange would ideally result in a signal exactly in between the intensity prior to bleach and that immediately after photobleach. But superimposed on this "fringe-mode" recovery is the "spot mode" that would occur without the Ronchi ruling, arising from exchange of molecules in the illuminated spot with the bulk solution. As the diffusion time varies with distance squared, the spot mode recovery will be much slower than the fringe mode recovery if several or more periods of the Ronchi pattern are illuminated. The intensity after photobleach is then

$$I_f(t) = B_i - \beta - \alpha \exp(-\Gamma t) + \delta t + \text{weaker terms} \quad (1)$$

B_i is the intensity prior to bleaching, or "base line". The rate $\Gamma = DK^2$ describes the fringe mode recovery, and $K = 2\pi/L$, with L the fringe periodicity spacing in the sample. The magnitude of the total perturbation in intensity is $\Delta = \beta + \alpha$. The term δt represents to first order the spot recovery mode. Typically $\delta \approx 0$, in which case $\alpha = \beta = \Delta/2$, assuming (as is actually the case) that the Ronchi rulings have exactly equal dark and bright stripes, that there are no immobile bleachable fluorophores, and that the bleach duration did not exceed about $0.1/\Gamma$. Bleach depth is usually such that $0.1B_i < \Delta < 0.3B_i$. The "weaker terms" in eq 1 include faster decay modes arising from interfringe exchange[7-9] and a more accurate representation of the slow spot recovery mode.[11] These terms are usually negligible, within experimental precision, but they can be removed completely by clever modulation detection schemes.[8-10]

TRFPR. Clearly, if any of the fluorescently tagged polymers are immobilized in a gel network, then complete recovery cannot occur. *Thus, incomplete recovery is a direct indicator of the existence of a gel network.* Moreover, the fraction, S, of labeled polymer in the sol phase is equal to the intensity recovery that occurs, divided by the maximum possible recovery, which is $\Delta/2$ for an ideal experiment employing a Ronchi ruling. The rate of whatever fluorescence recovery occurs yields the mobility of the sol-phase polymers through the gel network. After recovery stops, one may initiate a temperature ramp. When the temperature equals the gel melting point, the molecules trapped in the network are released, and the recovery proceeds further, the intensity approaching $B_i - \Delta/2$, neglecting spot mode recovery and convective motion. Since the distances over which the molecules must diffuse in order for this recovery to be detected are small (3–100 μm), the melting is detected almost immediately. This, plus the thin cell walls and small sample size, enables the temperature ramping to be relatively rapid. Altogether, the sol fraction, sol mobility, and melting point can be determined in less than 10 min.

Preliminary Measurements on Gelatin Gels. A description of the equipment, labeling procedure, and sample preparation has appeared.[12] Briefly, a technical grade of gelatin from MCB was labeled by adding fluorescein isothiocyanate (FITC), predissolved in acetone, to solutions in water. Care was taken to ensure that no free dye was present in the measured samples. The dye content is such that most gelatin chains do not contain even one dye moiety. Samples for TRFPR measurement were drawn into rectangular glass cells (0.1–0.3-mm path length) and allowed to gel while immersed in identical solutions, which were used for macroscopic observation.

Typical TRFPR traces from a labeled gelatin gel, such as Figure 1, adhere closely to the expected scenario, except for deviations due to convection at temperatures beyond the melting point. The sol fraction, S, is reasonably well-determined, and clearly the gel fraction $G = 1 - S$. A derivative plot, Figure 2, helps to identify T_{melt}. Figure 2 is reminiscent of a scanning calorimetry endotherm. However, the peak is directly associated with the disap-

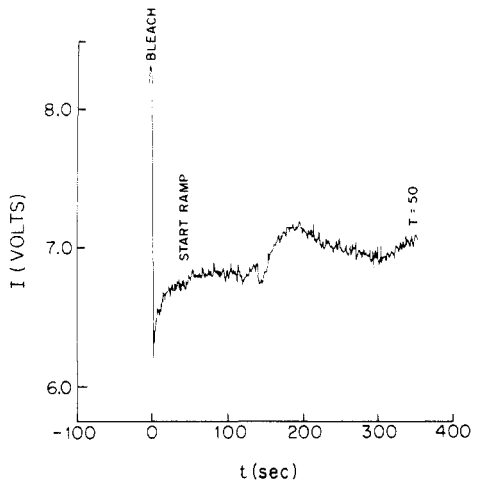

Figure 1. TRFPR trace for 4.94 wt % FITC-labeled gelatin gel.

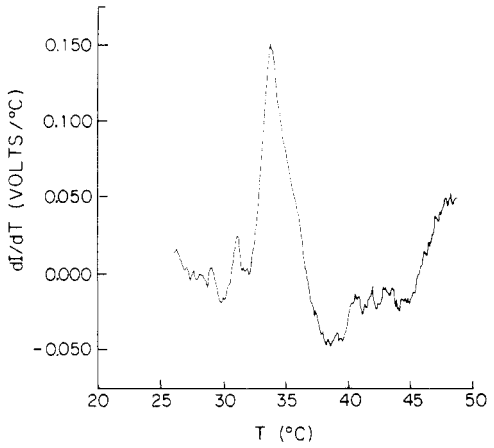

Figure 2. Derivative plot of temperature ramp for the same data as Figure 1, helping to identify the melting temperature.

pearance of the gel network, which need not be the case for the less direct calorimetric experiment. Also, a peak such as Figure 2 should be available even for reversible gels that have no heat of melting. The diffusivity, D, of the sol is obtained from the rate of partial recovery. For computational and display purposes, the recovery may be expressed as a decay of the perturbation caused by the photobleaching. Let $Y = |(\Delta - \beta)/\alpha|$ represent a normalized, decaying signal. A least-squares method was used to fit Y to an exponential decay, using fixed or floating β. The software can also account for the δt term of eq 1, but this wasn't necessary. As shown in Figure 3, the decays were single-exponential within error, with decay rate Γ. The diffusivity was directly obtained as $D = \Gamma/K^2$. To explore the possibility that nondiffusive recovery modes might interfere with proper diffusivity measurements, we have generated many Γ versus K^2 plots with the sodium salt of fluorescein in water[13] and also FITC-labeled gelatin in water, above its melting point. Such plots are inevitably straight lines with zero intercepts, within error, demonstrating the absence of any nondiffusive recovery mode (i.e., the photobleach is permanent).

Melting Points. In Table I, T_{visual} is the melting temperature measured by tilting the gels sideways in 13-mm test tubes and observing their shapes while raising the temperature at no more than 2 °C/h by increments of 0.5 or 0.25 °C. The general agreement with TRFPR is encouraging. However, the TRFPR melting points show slightly less variation with concentration than do the macroscopic values. This is sensible because gelatin gels are stabilized by a conformational transition, the temperature of which might be expected to be relatively independent of concentration. The systematic variation of the macroscopic melting points with concentration, as well as their slightly lower values, is attributed to perceived "flow" due to breakage of the macroscopic gels.

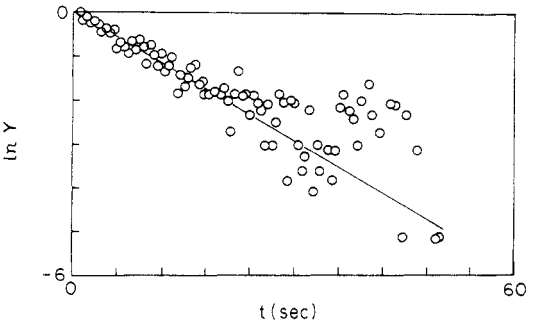

Figure 3. Isothermal recovery of intensity due to mobility of sol phase gelatin molecules, plotted as ln Y, where Y is the perturbation that was caused by photobleaching, normalized to span from 1 (corresponding to the initial large signal immediately after photobleaching) to 0 (corresponding to the intensity after recovery). Same data set as Figures 1 and 2.

Table I
Data Collected for a Series of Gels at Different Concentrations[a]

wt % gel	S/%	T_{melt}/°C (TRFPR)	T_{melt}/°C (visual)	$D/10^{-7}$ cm^2 s^{-1}
14.6	22 ± 7	31.7 ± 0.8	29.2_5*	2.11 ± 0.15
8.5	22	32.1 ± 0.3	28.5*	2.06 ± 0.55
4.94	40 ± 2	30.6 ± 0.1	27.5&	2.41 ± 0.25
1.94	100	NA	NA	2.58 ± 0.23

[a] All gels underwent identical treatment simultaneously: cool from 62 to ≈23 °C and age 1 day. Uncertainties are from repeat runs, except for visual melting, where uncertainties represent the temperature steps (* = ±0.5 °C; & = ±0.25 °C).

Sol Fractions. The sol fractions reported in Table I decrease monotonically as concentration increases. Even at high concentrations, a substantial portion of the gelatin retains mobility. The principle source of imprecision is uncertainty in estimating initial bleach depth. Potential inaccuracies include the need to assume that, at full recovery, the intensity would actually approach the ideal value, $B_i - \Delta/2$. For fully mobile solutions, this is the case if the photobleaching pulse is of sufficiently short duration and no extraneous, immobile bleachable fluorophores lie within the measurement volume (i.e., the sample, its cell, and the stage, which in our apparatus is not illuminated).

Diffusivities. There appears to be a slight decrease of mobility with increasing gelatin content. However, at all concentrations, the mobility of the sol phase is not dramatically different from that measured for the 1.94% solution, which was not a gel.

Discussion. What is certain is that TRFPR can be used to successfully measure true gel melting points and the mobility of the sol phase. The very existence of a gel, which in some systems is difficult to ascertain, is confirmed unambiguously by incomplete recovery of the FPR signal. The actual sol fraction is, at present, less well-determined. Although we are not aware of any comparably quantitative measurements of the sol fraction, we were still somewhat surprised by the high sol fractions reported herein. Several comments are pertinent to this observation.

(1) Gelatins vary widely with regard to source and preparation,[14] so our results could be specific to our sample. However, similarly high sol fractions have been observed with a second gelatin (a 300 Bloom pigskin gelatin from Aldrich). A highly purified, relatively monodisperse, and

well-characterized gelatin from a third source is being prepared.

(2) Measurements have been reported for just one set of conditions, for the sole purpose of demonstrating the technique. Yet the rate of gelation of gelatin is very sensitive to temperature and concentration.[15,16] Measurements without temperature ramping can be performed to follow the sol fraction during gelation, taking care to move the sample slightly between measurements so as not to bleach the same region twice. Such kinetic experiments, at several temperatures and concentrations, have been performed with the Aldrich pigskin gelatin just mentioned. At 25 °C it is observed that a measurable gel fraction exists within a few minutes, long before one would consider the macroscopic solution to be a "gel". The gel fraction does increase with time, although a substantial sol fraction remains even after 1 week at 10 °C. Improved precision would be highly desirable before extensive experiments along these lines are performed, but the preliminary results suggest that the existence of a substantial sol fraction is not completely an artifact of the TRFPR method itself, since the sol fraction decreases with time, which is the expected behavior.

(3) The gelatins studied so far are labeled so sparingly that an average chain does not even contain a dye moiety. This is good in the sense that the gelation characteristics of the system as a whole are probably not affected by dyeing. However, it is possible that a portion of the dyed molecules could be preferentially excluded from the network formed by the undyed molecules. This can be explored by varying the dye content.

(4) Gelatin is innately a polydisperse substance.[14] It is possible that the high sol fraction represents small gelatin fragments that were not incorporated into the gel structure. The positive side of this issue is that, given two sharp fractions, TRFPR could determine whether the incorporation of a polymeric species into the network depends on size. For example, a labeled low molecular weight polymer could be mixed with a larger, unlabeled fraction to determine whether and what percentage of the small molecules are incorporated into the network. No other technique for determining sol fraction with such selectivity is known.

(5) In determining the sol fraction, it is assumed that I_f is proportional to concentration. The concentration of dye in these experiments is very low ($<3 \times 10^{-5}$ mol dye/L at 10% gel). We have measured a linear relation between I_f and concentration in this range. However, for the strongly dyed gels required to test issue 3, the linearity would have to be reconfirmed. An advantage of modulation detection[8-10] is that very shallow bleaches can be used to create a measurable ac signal, eliminating this concern, even for the case of heavily dyed polymers.

(6) One may consider whether heating during the photobleaching pulse could cause partial melting of the gel, leading to high apparent sol fractions. Typically, the radiant power during photobleaches, averaged over the illuminated spot, is $\approx$200 cal/(cm^3·s). In the worst case, it is $\approx$750 cal/(cm^3·s), much higher than typical FRS measurements. In the present experiments, up to one-fourth of this energy may be absorbed, but as the quantum yield, Q, of fluorescein is thought to be about 0.90, and possibly almost unity,[17] most absorbed energy is reradiated. If $Q \approx 0.90$, temperature increases of approximately 20 °C/s would be possible in the case where there is a high degree of nonradiative deexcitation. However, this worst case seems not to materialize, since we have observed that the full power of the laser can be brought to bear on a gel at 25 °C indefinitely, creating a permanent, high-contrast fringe pattern, indicating no melting. Neither does performing the short (typically 250-ms) photobleaches at low temperatures far removed from T_{melt} result in lower sol fractions. In any event, the bleach pulses used for gels are similar to those for FPR in ordinary solutions where there is no indication that heating is a problem. The present methods require substantial bleach depths. Much shallower bleaches should be possible with modulation detection, because one need only create an ac signal, which may be reliably amplified, where there once was none. It will be interesting to see whether the apparent sol fraction remains similarly high when shallower bleaches are used.

Conclusion. That TRFPR can reliably measure melting points without mechanical perturbation is certain. Mobility of the sol fraction is also reliably obtained. The sol fractions measured so far are remarkably large, and the possible causes for this have been discussed. It is felt that sol fraction determinations will benefit greatly from modulation detection, which will enable more detailed studies. Even at present, however, the TRFPR and FPR methods are notable for the fact that they encourage difficult questions, such as the kinetics of sol fraction, to be pursued. Also, there appears to be no really better way to determine sol fractions, though the clever method of Fried and Bloomfield is certainly competitive.[18] This dynamic light-scattering-based method is, of course, completely free of mechanical and thermal perturbation, but it is slower, requires much more careful preparation of larger samples, a careful instrument calibration, and would not be easy to adapt for smooth temperature ramping to obtain melting points. Further refinements to the TRFPR and FPR methods should facilitate more detailed studies of a variety of reversible gels.

Acknowledgment. This study was partially supported by National Science Foundation Grant DMR-8520027 and by the Louisiana Stimulus for Excellence in Research. Helpful communications with Professor Hyuk Yu and Dr. Hongdoo Kim of the University of Wisconsin are gratefully acknowledged.

References and Notes

(1) Ferry, J. D. *Viscoelastic Properties of Polymers*, 3rd ed.; Wiley: New York, 1980; pp 537–9.
(2) Russo, P. S.; Mustafa, M.; Magestro, P.; Miller, W. G. In *Reversible Polymeric Gels and Related Systems*; Russo, P. S., Ed.; ACS Symposium Series 350, American Chemical Society: Washington, DC, 1987; Chapter 11.
(3) Tirrell, M. *Rubber Chem. Technol.* **1984**, *57*, 523.
(4) Chang, T.; Yu, H. *Macromolecules* **1984**, *17*, 115.
(5) Yoon, H.; Kim, H.; Yu, H. *Macromolecules*, in press. Also, private communication with H. Yu.
(6) Lee, J.; Kim, H.; Yu, H. *Macromolecules* **1988**, *21*, 858.
(7) Smith, L. M.; Parce, J. W.; Smith, B. A.; McConnell, H. M. *Proc. Natl. Acad. Sci., USA* **1979**, *76*(9), 4177.
(8) Lanni, F.; Ware, B. R. *Rev. Sci. Instrum.* **1982**, *53*(6), 905.
(9) Ware, B. R. *Am. Lab.* **1984**, *16*(4), 16.
(10) Davoust, J.; Deveaux, P. F.; Leger, L. *Eur. Mol. Biol. J.* **1982**, *1*, 1233.
(11) Axelrod, D.; Koppel, D. E.; Schlessinger, J.; Elson, E.; Webb, W. W. *Biophys. J.* **1976**, *16*, 1055.
(12) Russo, P. S.; Mustafa, M.; Tipton, D.; Nelson, J.; Fontenot, D. *Polym. Mater. Sci. Eng.* **1988**, *59*, 605.
(13) By such methods, we establish the self-diffusivity of sodium fluorescein in pure water at 25 °C as $(5.1 \pm 0.2) \times 10^{-6}$ cm^2/s.
(14) Veis, A. *The Macromolecular Chemistry of Gelatin*; Academic Press: New York, 1964.
(15) Djabourov, M.; Leblonde, J. In *Reversible Polymeric Gels and Related Systems*; Russo, P. S., Ed.; ACS Symposium Series 350; American Chemical Society: Washington, DC, 1987.
(16) (a) Djabourov, M.; Leblond, J.; Papon, P. *J. Phys. (Les Ulis, Fr.)* **1988**, *49*, 319. (b) Djabourov, M.; Leblond, J.; Papon, P. *J. Phys. (Les Ulis, Fr.)* **1988**, *49*, 333.

(17) Demas, J. N.; Crosby, G. A. *J. Phys. Chem.* **1971**, *75*(8), 991.
(18) Fried, M. G.; Bloomfield, V. A. *Biopolymers* **1984**, *23*, 2141.

Mazidah B. Mustafa, Debbie Tipton, and Paul S. Russo*

Macromolecular Studies Group and Department of Chemistry, Louisiana State University Baton Rouge, Louisiana 70803-1804

Received September 29, 1988; Revised Manuscript Received December 27, 1988

Mixed-Integer and Fractional-Integer Chain Folding in Crystalline Lamellae of Poly(ethylene oxide): A Raman Longitudinal Acoustic Mode Study

Observations of stepwise increases in SAXS lamellar spacings of low molecular weight poly(ethylene oxide) (PEO) fractions as a function of crystallization temperature[1] and annealing temperature,[2] as well as detailed studies of growth rates and morphologies,[3-6] have led to the concept of integer folds (IF) in these systems, viz., chain folds for which all stems of a molecule are of the same length with chain ends located at the lamellar surfaces. Early Raman longitudinal acoustic mode (LAM) studies of PEO[7] also gave evidence for such IF structures, as have recent transmission electron microscope studies.[8] Similar IF structures have been proposed for ultralong *n*-paraffins.[9]

In all of the above PEO studies, it has been assumed that, for a given polymer and crystallization condition, the lamellae are homogeneous and contain only single IF structures. Our LAM studies of PEO, together with DSC and SAXS data, suggest that there are lamellae that contain a mixture of IF structures as well as lamellae that are comprised of chains with simple fractional-integer folds (FIF). We believe that such FIF are also indicated by results on ultralong *n*-paraffins,[10,11] although the SAXS data[11] were interpreted in terms of general noninteger folds.

The LAM frequency, ν, can be used to determine the ordered length, L, of a polymer chain stem in a crystalline lamella. However, the value obtained for L depends on the assumptions made in relating ν to L: for an unperturbed elastic rod model, $\nu = (1/2L)(E/\rho)^{1/2}$, where E is the elastic modulus and ρ is the density of the rod. For the general perturbed composite elastic rod, more complex relationships hold,[12,13] and if the polymer stem is treated at a molecular rather than a continuum level, the detailed effects of perturbations can be elucidated only by normal mode analyses.[14]

We have refined a force field for PEO that includes intermolecular interactions explicitly and have used it in normal mode calculations of LAM frequencies of extended-chain oligomers.[15,16] We find that, in distinction to the case of planar zigzag polymethylene chains, the LAM of helical chains is affected significantly by lateral interactions. This force field was used to calculate LAM frequencies of folded-chain PEO molecules and to interpret Raman spectra of a series of PEO fractions crystallized under different conditions.[16] Some of these results are presented here.

We consider first the case of a PEO fraction of $M = 3000$ ($M_n = 3336$, $M_w/M_n = 1.10$). In Figure 1 are shown the LAM spectra and DSC curves (obtained at 5 °C/min) for room-temperature crystallization, T_c = RT (RT = room temperature) (crystallization time t_c = 1 day), and T_c = 55 °C (t_c = 5 days) samples. The SAXS patterns of these samples show 3 orders of both a 128-Å and a 107-Å spacing for the T_c = RT sample and at least 6 orders of a 214-Å spacing for the T_c = 55 °C sample. The LAM bands at 5.5 and 11.6 cm^{-1} for the T_c = 55 °C sample correspond to stem lengths of 204-Å (i.e., extended (E)) and 102-Å (i.e., once-folded (F2)) molecules, respectively[16] (the band near 19 cm^{-1}, found in all PEO samples, is a lattice mode[16]). The LAM bands at ~9.5 and 11.6 cm^{-1} for the T_c = RT sample correspond to stem lengths of ~122 and 102 Å, respectively.

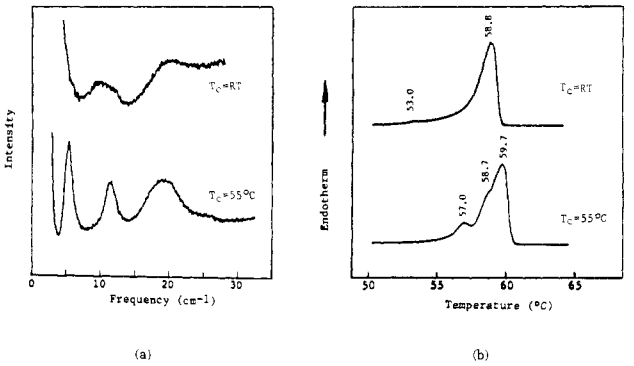

Figure 1. (a) Low-frequency Raman spectra and (b) DSC melting curves of PEO 3000 crystallized at different crystallization temperatures (T_c).

For the T_c = RT sample, the 11.6 cm^{-1} LAM band and the 107-Å SAXS spacing clearly indicate the presence of independent lamellae of once-folded molecules, i.e., monolayer, F2(M), lamellae (the stem length of such chains, assuming a "tight" fold containing three EO units, is expected to be 101 Å). On heating in the DSC, such lamellae (with melting temperature $T_m \cong 53$ °C[17,18]) are expected to be unstable, and we believe that they convert to bilayer, F2(B), lamellae with observed T_m = 58.8 °C (Figure 1). The other LAM and SAXS spacings, viz., 122 and 128 Å, respectively, are consistent with an F1.5(M) lamella;[16] since the length of the molecule is 211 Å, we presume that in this case the fold is relatively "loose" and that chain ends can emerge from the surface as cilia. Such a lamella would also be expected to be unstable and not show up as a separate peak on heating in the DSC. (We also deduce the presence of FIF chains from an analysis of the LAM spectra of a M = 10 000 PEO sample.[16]) Letting crystallization proceed to t_c = 45 days, we find LAM peaks at 7.5 and 11.6 cm^{-1}, and the 128-Å spacing almost disappears as a 214-Å spacing becomes evident;[16] these changes, plus the DSC scan, can be interpreted in terms of the presence of F1.33(B) and F2(M) chains.[16]

For the T_c = 55 °C sample, the 5.5-cm^{-1} LAM band, the 214-Å SAXS spacing, and the expected 211-Å extended chain length are all consistent with the prescence of E lamellae, as are the T_m of 59.7 °C[17,18] and the T_c[3] (the T_m = 57.0 °C peak in the DSC is probably due to some fractionated species[16]). However, the presence of a LAM peak at 11.6 cm^{-1}, resulting from F2 stems, is not expected at this T_c[3]. The location of such F2 molecules is also not clear; some could be in separate F2(B) lamellae, which is suggested by the shoulder in the DSC at 58.7 °C; however, in view of the relative intensities of the LAM and DSC peaks, we should not exclude the possible presence of F2(B) structures within E lamellae.

We turn now to results on a PEO fraction of M = 5000 (M_n = 4506, M_w/M_n = 1.10). In Figure 2 are shown LAM spectra and DSC curves for T_c = RT, 46 °C, and 58 °C samples, all for t_c = 5 days. The SAXS patterns of these samples show spacings of 136 Å (4 orders), 269 Å (6 orders), and 273 Å (6 orders), respectively. The LAM bands of these samples are at 8.5, 8.7, and 3.9, 8.7, and 13.5 cm^{-1}, respectively, the latter three peaks corresponding to stem

0024-9297/89/2222-1504$01.50/0